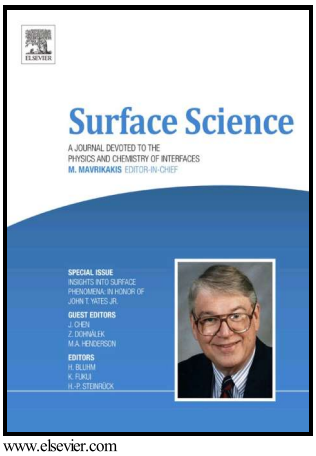

www.elsevier.com

LEED – IV and DFT study of the co-adsorption of chlorine and water on Cu(100)

M. Puisto, K. Pussi, M. Alatalo, D. Hesp, V.R. Dhanak, C.A. Lucas, Y. Grunder

PII: S0039-6028(16)30319-3
DOI: http://dx.doi.org/10.1016/j.susc.2016.11.005
Reference: SUSC20959

To appear in: *Surface Science*

Received date: 14 July 2016
Revised date: 9 October 2016
Accepted date: 5 November 2016

Cite this article as: M. Puisto, K. Pussi, M. Alatalo, D. Hesp, V.R. Dhanak, C.A Lucas and Y. Grunder, LEED – IV and DFT study of the co-adsorption of chlorine and water on Cu(100), *Surface Science* http://dx.doi.org/10.1016/j.susc.2016.11.005

LEED – IV and DFT study of the co-adsorption of chlorine and water on Cu(100)

M. Puisto[1], K.Pussi[1], M. Alatalo[1,2], D. Hesp[3], V.R. Dhanak[3], C.A. Lucas[3], Y. Grunder[4]

[1] *LUT School of Engineering Science, Lappeenranta University of Technology, P.O. Box 20, FIN-53851 Lappeenranta, Finland*

[2] *Theoretical Physics Research Unit, University of Oulu, P.O. Box 8000, FI-90014 University of Oulu, Finland*

[3] *Department of Physics, University of Liverpool, Liverpool, L69 3BX, UK*

[4] *School of Chemistry, The University of Manchester, Oxford road Manchester, M13 9PL*

Abstract

We have studied the adsorption of water on a Cl covered Cu(100) surface using both low energy electron diffraction (LEED) experiments and density functional theory (DFT) calculations. On the Cu{100}-c(2×2)-Cl surface water is shown to form a bilayer, which is weakly bound to the surface.

Keywords: LEED, DFT, Adsorption, Cu, Cl, water

1. Introduction

In many technologies the structure of an electrode electrolyte interface is of interest as modifying catalysts to improve their performance is a goal of several fields of industry. Both experimental and theoretical studies have thus been performed to understand water adsorption from a fundamental level. The adsorption of water on single crystal metal systems has been explored previously and several reviews can be found in the literature [1, 2, 3, 4]. On some hexagonal surfaces water has been observed to form an ice-like bilayer [3, 4]. When the kinetics allow it, however, there were no overlayer structures observed on surfaces with a square symmetry. When bound to metal surfaces water is found to prefer sites with a higher electron density as it is usually through the oxygen atom that the water molecules interact

with the surface. This interaction has been found previously to be a weak one, comparable in strength to the hydrogen bonding between adjacent water molecules in an overlayer structure. Due to the weak nature of this interaction the electronic structure of the substrate is mainly unperturbed [5]. Upon adsorption of water molecules, a reduction in the value of the work function occurs due to their dipole nature.

Halogens adsorbed on metals are known to inhibit catalytic reactions by blocking reactive species, i.e. cations. At the electrochemical interface, where reactions take place in an aqueous environment, understanding how the presence of water perturbs the substrate is of fundamental interest. When chlorine gas is adsorbed on metals a strongly bound stable adsorbate system is produced [6]. This system has been studied previously on Cu(100) in both Ultra High Vacuum [6, 7, 8] and electrochemical systems [9]. LEED IV studies found that chlorine forms a c(2×2) chemisorbed layer on Cu(100) with p4mm symmetry, the Cl atoms occupying the energetically favourable fourfold hollow sites [6].

Conventionally, the first wetting layer on a close-packed metal surface (the classic bilayer) is a single (0001) sheet of ice, strained to achieve $(\sqrt{3} \times \sqrt{3})$ R30 periodicity. The bilayer model has two water molecules in a unit cell, one lies almost parallel to the metal surface, binding to it through an oxygen lone-pair orbital, and the other lies several tenths of an Å higher, contributing one O-H bond to the interlayer H-bond network, while the other bond dangles into the vacuum. [1] The O-O distance in hexagonal ice is 2.75 Å.

In this study we adsorb water molecules onto the c(2×2) structure and determine what effect the water molecules have on the initial system. We examine the structure of the system using LEED IV analysis and probe the overall energy and charge transfer of the system by means of a DFT study. Water does not adsorb to this system at room temperature and so the system was cooled to 133 K to be studied. Water adsorption on Cu{100}-Cl template is more complicated because of the [U+201C]square[U+201D] periodicity of the substrate. Cl atoms take 2×2 periodicity and sit at hollow sites [10]. Cl-Cl distance is 3.61 Å (100-direction) or 5.11 Å (110- direction). Because the desired O-O distance for the water layer is 2.75 Å, one water molecule per unit cell is not enough if we assume water- water interaction. So the structure most likely has two water molecules per unit cell. This means that the O atoms of different water molecules can not reside in a single layer. In (100)-direction the corrugation of the water layer needs to be about 2 Å, in (110)-direction about 1 Å is needed. The corrugation of the

substrate in (100)-direction is about 1.8 Å and in (110)-direction about 1.8 / 3.5 Å depending on the path chosen. If one makes an assumption that the corrugation of the water layer follows the corrugation of the substrate, then the (100)-direction would be more favorable. At non-hexagonal surface the resulting structure will be a consequence of the balance between water-water and water-metal interactions, which makes it difficult to make any structural predictions.

2. Methods

2.1. Experimental

The experiments were performed in a standard Ultra High Vacuum surface science chamber consisting of a PSP vacuum technology electron energy analyser, a dual anode x-ray source, a helium 1 Ultra-Violet Lamp and a rear-view LEED optics from OCI Vacuum Microengineering. The LEED measurements were done using an MCP LEED optics with a very low beam current. The MultLEED software package was used to extract the intensities of the LEED images. The base pressure of the system was less than $2 \cdot 10^{-10}$ mbar with hydrogen as the main residual gas in the chamber. The Cu(100) crystal was prepared by cycles of argon ion bombardment and annealing to 870 K, the sample was then considered clean when a sharp LEED pattern was observed and the XPS scans showed no traces of contamination. Chlorine was deposited onto the system at room temperature using an electrochemical cell as described in Ref. [11]. From previous work it is known that chlorine forms a 2×2 structure on the Cu(100) surface. It was also found that the sticking fraction drops to almost zero after the 2×2 structure is formed all over the surface [7], therefore chlorine was dosed until a sharp c(2×2) LEED pattern was observed which corresponds to a coverage of 0.5 monolayers. The LEED spots, with similar order of magnitude for integer and half order beams are sharp with a low background, typical of well-ordered long range domains [8]. Water was dosed onto the sample via a leak valve whilst the sample was cooled to 133 K. At room temperature water did not adsorb to the system. This was noted by examining the XPS and UPS spectra which showed no oxygen peaks growing after dosing. 15 Langmuirs of water were deposited at a pressure of $1.3 \cdot 10^{-7}$ mbar for 150 seconds. The sample was cooled via a cooling block attached to the sample mount, nitrogen is flown through this copper block cooling the sample, the sample was allowed to cool for 15 minutes before dosing the water to ensure it had reached the desired

temperature. The XPS scans showed the interaction of the water with the underlying system to be weak. The oxygen peak in the XPS scans indicates the presence of the water as well as the change in work function which was observed upon adsorption. The work function change was calculated from examining the valence band using UPS.

2.2. LEED + DFT Method

The dynamical LEED calculations were performed using the Tensor-LEED program [12]. The relativistic phase shifts were calculated using the phase shift program [13] that is packaged with Tensor-LEED. The agreement between the theory and the experiment was tested using the Pendry R-factor and the error bars quoted are calculated using the Pendry RR-function [14].

The spin polarized calculations were performed at the level of Density Functional Theory (DFT) applying the Vienna Ab-initio Simulation Package (VASP) [15, 16, 17, 18], with the PBE exchange-correlation [19]. The van der Waals interactions [20] were included as suggested in [21, 22], later referred to as vdW-DF2. 600 eV was chosen as the appropriate cut-off for the plane-wave expansion of the electron wave functions. The k-point sampling followed a two-dimensional 11×11×1 Monkhorst-Pack mesh [23].

The surface slab consisted of nine layers of Cu, each layer having periodically continuous plane direction. In the off-plane direction, a vacuum of 30 Å was utilized between each slab. For the PBE, the lattice parameter of 0.364 nm was obtained for bulk Cu using these computational approximations. For the vdW-DF2, the lattice parameter was 0.369 nm, while the experimental value is 0.361 nm [24]. The slight overestimation of the lattice pareameter is typical for DFT calculations using generalized gradient approximations. Also it is well known that vdW-DF2 tends to overestimate the lattice constant for the transition metals, ionic solids, and semiconductors, while the lattice parameters for the alkali and alkali-earth are underestimated [25].

Cu(100) has three high symmetry adsorption sites: Top (T), bridge (B), and hollow (H). Chlorine was calculated to prefer the hollow site for both with and without the vdW-DF2. For the PBE, the adsorption simulations were performed with parallel and tilted mode of water so that over 50 positions were studied.

3. Results

3.1. LEED I(E) analysis

3.1.1. Cu{100}-c(2×2)-Cl

The adsorption site for Cl on Cu{100} was confirmed using a data set of 5 beams (3 integer and 2 fractional order beams), ranging from 20 eV to 420 eV, recorded at 300 K. The cumulative energy range is 1600 eV. Three different sets of phase shifts were used; one for Cl, one for top layer copper atoms and one for the copper atoms in deeper layers. At the beginning of the analysis the Debye temperatures were set to 500 K and 343 K for Cl and Cu respectively, lmax value was set to 8 and the imaginary part of the inner potential was set to -5 eV.

At the first stage of the analysis the high symmetry adsorption sites were considered and it was very clear that the hollow site is the correct adsorption site for Cl as was stated in reference [6].

The final refinement of geometrical and non-structural parameters reduced the R-factor for the hollow site down to 0.17. The final structural and non- structural parameters are listed in table 1 and the I(E) curves for the optimum structure are shown in figure 1.

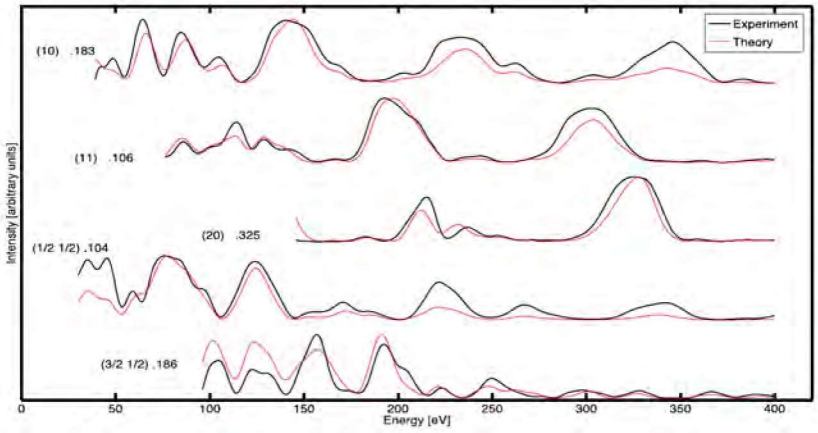

Figure 1: I(E) curves for the best fit Cu{100}-Cl structure.

3.1.2. Cu{100}-c(2×2)-Cl + H_2O

The data set utilized consisted of 5 beams (3 integer and 2 fractional order beams), ranging from 20 eV to 420 eV, recorded at 133 K. The cumulative

Parameter	value
dz(Cu-Cl)	1.62 Å
dz(Cu_1-Cu_2)	1.82 Å
dz(Cu_2-Cu_3)	1.81 Å
dz(Cu_3-Cu_4)	1.80 Å
dz(Cu_4-Cu_5)	1.79 Å
dz(Cu_5-Cu_6)	1.83 Å
δ_1	0.00 Å
δ_2	0.00 Å
δ_3	0.00 Å
δ_4	0.03 Å
δ_5	0.00 Å
Θ_DCl	360 K
Θ_DCu(surface layer)	300 K
Θ_DCu(bulk	343 K
I_{max}	10
V_i	-5 eV
dz(bulk)	1.805 Å

Table 1: Structural and non-structural parameters for the best fit structure of the Cu-Cl system. dz=interlayer spacing calculated between the centers of mass of Cu atoms, δ_i = average buckling within each copper layer, ΘD is the Debye temperature and V_i the imaginary part of the inner potential.

energy range is 1600 eV. Six different sets of phase shifts were used; two for oxygen, one for hydrogen, one for Cl, one for top layer copper atoms and one for the copper atoms in deeper layers. At the beginning of the analysis the Debye temperatures were set to 500 K, 500 K and 343 K for O, Cl and Cu respectively, lmax value was set to 8 and the imaginary part of the inner potential was set to -5 eV. These values were optimized at the final stage of the analysis. The real part of the inner potential is independent of energy and it is allowed to relax as is the normal procedure in the LEED analysis.

Because LEED is not very sensitive to the light H atoms and the length of the data set was limited, the H atoms were ignored in the analysis. DFT

results and [U+201C]unit cell dimensions[U+201D] suggested that the water coverage should be two water molecules per unit cell. However in the LEED analysis both the one molecule and two molecule cases were considered. The adsorption geometries were chosen by using the high symmetry adsorption sites of the substrate unit cell (top-Cu, top-Cl, hollow and bridge) and different combinations of those sites. At this stage of the analysis the O atoms and the Cl atom, and the top layer substrate atoms were optimized vertically (z-coordinate). The model structures were not restricted by any symmetry. Domain averaging was used for those trial structures that had lower symmetry than the c(2×2) observed in the LEED experiment.

At later stage the non-structural parameters were optimized for the most promising model structures (top Cu, top Cl, bridge, top Cu + top Cu and top Cl + top Cu). Out of the single molecule adsorption geometries left at this stage the bridge site gave an unphysical result; a very short O-Cl distance of 1.32 Å was found. Thus this geometry was discarded from the LEED I(V) analysis. The on top Cu model structure is very similar to the two molecule version of this model with both oxygen molecules on top of Cu. Since DFT indicated that the models with two water molecules are more stable, the rest of the effort has been concentrated on two molecule models.

Out of the two models that have two water molecules in the unit cell the model with one oxygen on top of Cl and one on top of Cu had again a very short O-Cl distance of 1.62 Å So out of the four models that have very similar R-factors in table 2, only the model with both oxygen atoms on top of Cu needs to be considered for final refinement. As a final refinement lateral relaxation was allowed for the top layer Cu atoms, the Cl atom and the two oxygen atoms.

The best fit geometry has the two O atoms almost on top of the top layer copper atoms, at two different levels. The final Pendry R-factor is 0.26. The optimized structural and non-structural parameters are listed in table 3. Top and side views of the best fit geometry are shown in Figure 2 and Figure 3 shows the I(E) curves for the optimum structure.

The general features in the LEED and DFT results compare well. In DFT the water chains are straighter whereas in LEED the water chains are more zig-zag shaped. The oxygen-oxygen bond length is in good agreement with the O-O bond length in hexagonal ice (2.75 Å) for both DFT (2.64 Å) and LEED (2.5[U+00B1]0.2 Å). The underlying Cu-Cl substrate remains unchanged for both cases, when compared with the structure of Cu-Cl before water adsorption.

Adsorption cite	Pendry R-factor
top Cu	**0.28**
top Cl	0.34
bridge	**0.31**
top Cu + top Cu	**0.28**
top Cl + top Cu	**0.31**

Table 2: R-factors after refining the non-structural parameters for H_2O adsorption on Cu{100}-Cl surface. After this stage all models having R-factors above 0.32 can be discarded (Pendry RR-factor is 0.04). The models that have to be considered for further analysis are indicated with bold font.

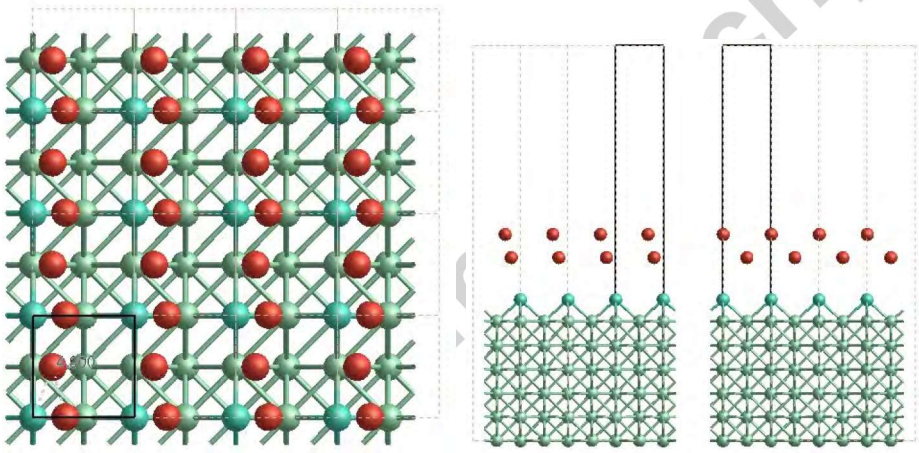

(a) (b)

Figure 2: Top (a) and side (b) views of the best fit Cu{100}-Cl + H_2O structure. The red spheres represent oxygen, green ones copper, and the turquoise ones chlorine.

The LEED result is heavily steered by the DFT analysis. During the LEED analysis multiple minima with very similar R-factors (R-factors between 0.25- 0.30) were discovered. The main features, such as the preference

Parameter	Value
NN O-Cu	4.9±0.2Å
NN O-Cl	3.7 ±0.2Å
NN O-O	2.5 ±0.2Å
dz(O-O)	1.8 ±0.2Å
δO	0.7/1.2 ±0.2Å
dz(Cl-Cu)	1.64 ±0.03Å
dz(Cu1-Cu2)	1.84±0.03Å
dz(Cu2-Cu3)	1.83±0.03Å
dz(Cu3-Cu4)	1.81±0.05Å
dz(Cu4-Cu5)	1.79±0.07Å
dz(Cu5-Cu6)	1.79±0.13Å
δ_1	0.01±0.04Å
δ_2	0.00±0.02Å
δ_3	0.02±0.04Å
δ_4	0.03±0.05Å
δ_5	0.05±0.10Å
Θ_DO(upper)	110 K
Θ_DO(lower)	90 K
Θ_DCl	210 K
Θ_DCu(surface layer)	210 K
Θ_DCu(bulk)	343 K
l_{max}	12
V_i	-6.5 eV

Table 3: Structural and non-structural parameters for the best fit structure of Cu-Cl-H_2O system. dz=interlayer spacing calculated between the centers of mass of Cu atoms, δ= average buckling withing each copper layer, Θ_D Debye temperature, V_i imaginary part of inner potential, δ_O = lateral relaxation of the O atoms away from the topCu-Cl row and NN = nearest neighbor distance.

for almost on top Cu site adsorption and formation of oxygen chains along the (100) direction, for these structures were comparable with each other. However some important details seemed almost irrelevant from the point of

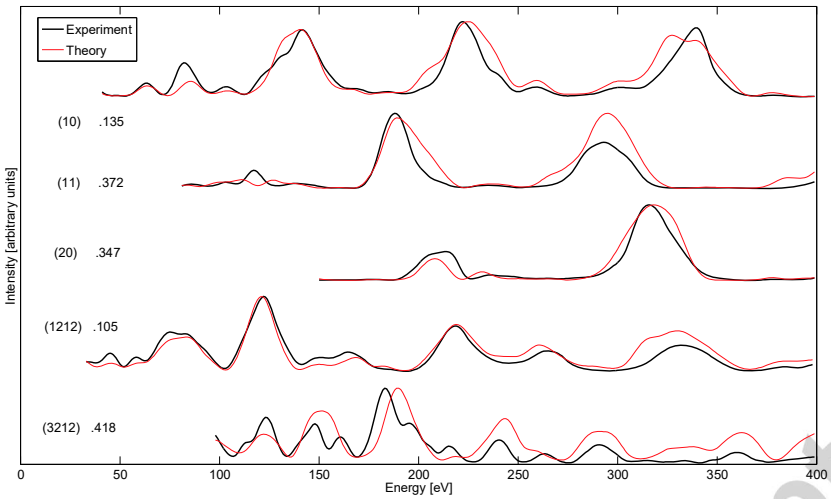

Figure 3: I(E) curves for the best fit Cu{100}-Cl + H_2O structure.

view of the R-factor, for example the vertical distance between the oxygen atoms and the substrate top layer copper. This is in a way surprising, since LEED is known to be most sensitive to the parameters in vertical direction.

3.2. DFT Results

3.2.1. Water adsorption on Cu{100}-c(2×2)-Cl

Out of a large number of different model structures, three main structures could be identified, which all have very similar adsorption energy (see Figure 4 and Table 4). These structures were chosen for closer study with and without the van der Waals interaction. The water layer consists of "chains" of water, where the water molecules alternate at two different levels. The vertical separation of the water molecules is about 1.9 Å for the PBE and 2.0 Å for the vdW-DF2. The bonds and angles in the water chains are very similar in each structure type. The lower H atom of the upper water molecule points towards the oxygen atom of the lower water molecule and the upper H atom of the lower water molecule points towards the oxygen of the next upper water molecule. Both water molecules thus have one hydrogen that is involved in the formation of the water chain and the other hydrogen is pointing towards the substrate (lower molecule) or towards vacuum (upper molecule). For the PBE, the vertical distance between the water chains and substrate varies between 4.76-5.75Å and for the vdW-DF2 it varies between 4.84-5.12Å for the

different models. The nearest neighbor bond lengths between the substrate atoms and atoms in the water layer vary a little depending on the position of the water chain with respect to the substrate. The main difference between the three structure types is the orientation of the H atoms with respect to the substrate. Table 4 lists the interaction energy between the water layer and the surface, and the nearest neighbor distances for each structure type. For these results, we consider the water layer – surface interaction. This interaction energy is calculated by subtracting the sum of total energies of isolated water layer and substrate from the total energy of the combined system [26]. More detailed information on the bond lengths for one structure is given in Table 5.

Structure type	Type of calculation	Interaction energy [eV]	NN Cl-O [Å]	NN Cl-H [Å]	NN O-O [Å]	δO [Å]
(a)	PBE	-0.02	3.63-3.82	2.89-3.20	2.64	1.17-1.36
	vdW-DF2	-0.09	3.59	2.73	2.70	1.54
(b)	PBE	-0.01	3.73-3.84	3.43-3.68	2.64	0.39-0.67
	vdW-DF2	-0.07	3.45	3.15	2.73	0.49
(c)	PBE	-0.02	3.77-4.17	3.04-3.70	2.64	1.72-1.84
	vdW-DF2	-0.12	3.50	2.76	2.71	1.66

Table 4: Interaction energy of a water layer on Cu(100)-Cl. Letters (a), (b) and (c) correspond to models shown in Figure 4. NN = nearest neighbor and δO is the lateral distance of the O atoms from the topCl-topCu line (shown in Figure 4).

The water chains can move with respect to the substrate as long as the chains are aligned with the (100)-direction. Therefore, our interpretation is that the water-substrate interaction is very weak. The dominating interaction in this system is the water-water interaction within the water chains. For the PBE, the binding energy of the water chains is -0.37 eV/H_2O for all configurations. For vdW-DF, the binding energy is -0.38 eV/H_2O eV for type C configuration and -0.39 eV/H_2O for type A and B configurations. For comparison, the experimental value for the hexagonal ice is -0.61 eV/H_2O [27].

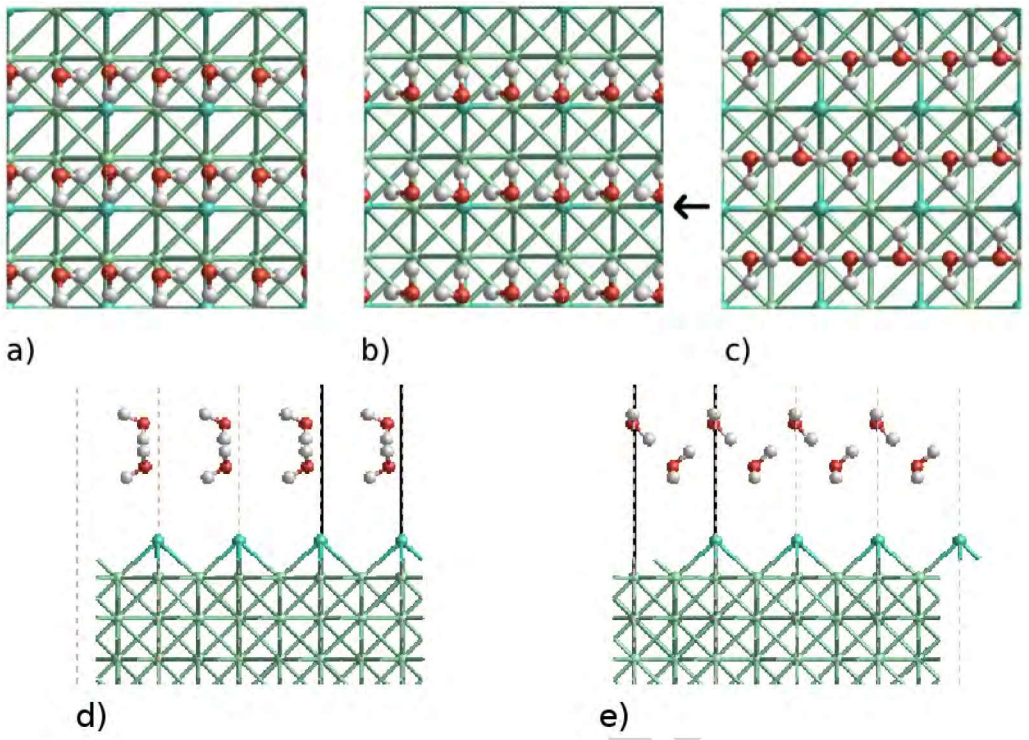

Figure 4: Top and side views for the best fit models calculated by DFT. Different structure types are: (a) Hydrogens oriented towards topCu-Cl row, (b) oxygens towards topCu-Cl row and (c) hydrogens alternate from side to side. Black arrow indicates the position of the topCu-Cl row. Figures (d) and (e) are side views of figure (c). The red spheres represent oxygen, white ones hydrogen, green ones copper, and the turquoise ones chlorine.

The alignment of the water chains is probably steered both by the Cl atoms and by the dimensions of the 2×2 unit cell. The underlying substrate remains almost unchanged, the copper interlayer spacings have surface-like values and the Cl remains at the same position as it was before the adsorption of water.

Figure 5 shows the interaction energy, calculated with and without the vdW-DF2 implementation, for the water layer approaching the Cu/Cl surface. For the PBE, the steady state distance for the adsorbed water layer is at 5 Å above the topmost Cu corresponding to the interaction energy of -0.02 eV. For the vdW-DF2, the calculated steady state distance for the adsorbed

Parameter	PBE	vdW-DF2
NN(H-Cl)	2.985 Å	2.733 Å
NN(H-O)	0.975 Å	0.976 Å
∠(H-O-H)	105.773°	105.785°
∠(H-O-H)	105.642°	105.449°
NN(O-O)	2.637 Å	2.701 Å
dz(O-O)	1.93 Å	2.00 Å
NN(O-Cu)	5.142 Å	4.837Å
NN(O-Cl)	3.713 Å	3.585 Å
dz(Cl-Cu)	1.66 Å	1.70 Å
δO	1.17/1.30 Å	1.41/1.67 Å

Table 5: Numerical data about bonds and angles in one structure that belongs to structure type (a) calculated with and without the vdW-DF2. δO = lateral relaxation of the O atoms away from the topCu-Cl row, dz is the vertical distance of atoms and NN = nearest neighbor distance.

water layer is at 4.5 Å above the topmost Cu. The interaction energy between the surface and water layer is -0.12 eV. Comparing the two interaction curves demonstrates that the non-local van der Waals interactions drive the adsorption process starting already from distances of around 6 Å above the Cu surface layer. The potential between the surface and the water layer is highly asymmetric around the potential energy minimum: Decreasing the water layer – surface distance results in rapidly increasing repulsive interaction, whereas at higher distances the potential is behaving more smoothly, finally settling at 8 Å to the vacuum state.

To understand the properties of water layers on the Cu{100}-c(2×2)-Cl surface, the local electronic structures of each contributing atom are carefully analyzed. Figures 6 and 7 show local densities of states (LDOS) calculated with the PBE and the vdW-DF2 for the most stable calculated structure, in which the hydrogens are oriented towards topCu-Cl row. Figures 6 (a) and 6 (b) show the s- and p-orbitals for oxygen of the H_2O molecule in vacuum and on a Cu-Cl surface. Figures 6 (c) and 6 (d) show the s- and p- orbitals for Cl with and without the water layer, and figure 6 (e) and 6 (f) show the LDOS

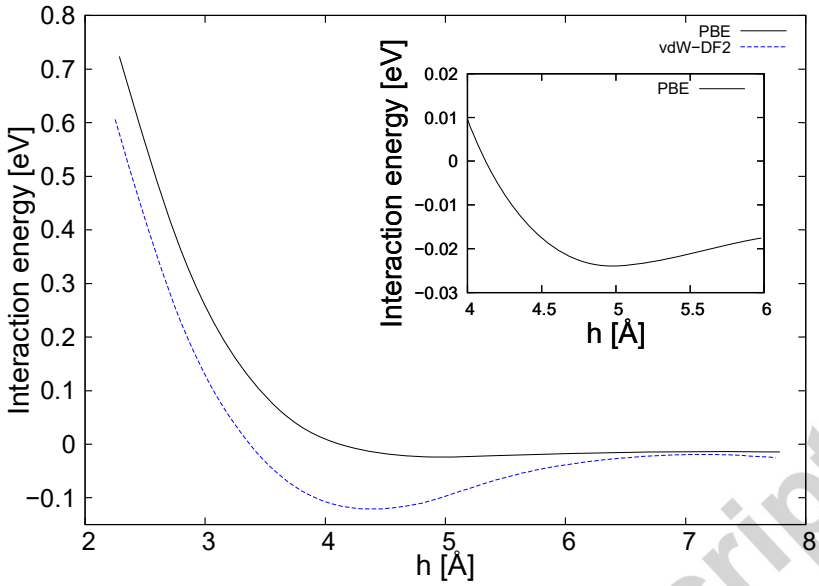

Figure 5: The PBE and vdW-DF calculated interaction energy for a water layer approaching the Cu(100)-Cl surface. The distance between the lowermost oxygen atom of the water layer and the closest Cu layer of the surface is named h. The oxygen-Cu(100)-Cl surface distances were kept fixed during the calculations, while the rest of the system was allowed to relax. Inset: A detail around the equilibrium height, showing a weak minimun at 5 Å for the PBE

of Cu, closest to the Cl with and without the water layer. Comparison of the oxygen atom LDOS in figures 6 (a) and 6 (b) indicates that the shape of the second peak on p-orbital changes slightly. The changed shape indicates that the oxygen in the water molecule interacts with the surface. The fact that the maximum density of the oxygen s- and p-LDOS shifts about -2.5 eV below E_f orbitals is because the surface defines the Fermi energy for LDOS(b) and the LDOS(a) is calculated without the presence of surface.

The Bader charge analysis [28, 29, 30, 31] results for the PBE calculations are presented in the supplementary material. According to the analysis, the charge transfer from the surface to the water layer is negligible for all configurations. Comparing the water layer covered system and the pure water layer, the difference in the water layer charge is less than 0.01 regardless of the use of the vdW-DF2. According to Ref. [28] this can be regarded as an error bar for the Bader analysis. The water layer therefore has no electron transfer

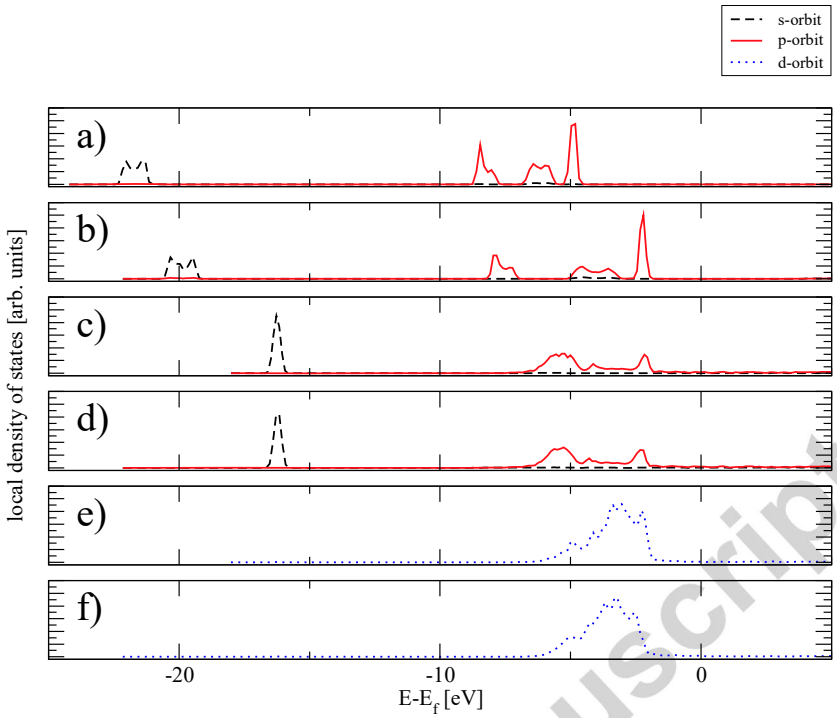

Figure 6: The density of states (LDOS) calculated with the PBE, for the most stable, type C structure, in which the hydrogens are oriented towards the top Cu-Cl row. The plots show the LDOS for a) and b) the oxygen of the H_2O molecule, c) and d) LDOS for the Cl atom, and e) and f) LDOS for the nearest Cu atoms, without and with the water dimer – surface interaction.

from the surface. The chlorine charge does not depend on the presence of the water layer on the PBE calculated system. On the other hand, comparison of the chlorine charge between the water layer covered system and the separately calculated water layer shows some difference for the vdW-DF2 calculation. For type A and C the chlorine charge difference is about 0.03 electrons and for type B configuration about 0.04 electrons. The modest charge transfer between the water layer and the Cl ad-atom indicates a very weak interaction between the water layer and the surface.

In order to see how the Cl layer affects the interaction energy, the calculations were performed at the same parameters as before, but without Cl. The relaxed structures are presented in figure 8. One should note that a detailed analysis of these structures is likely to require a larger supercell than

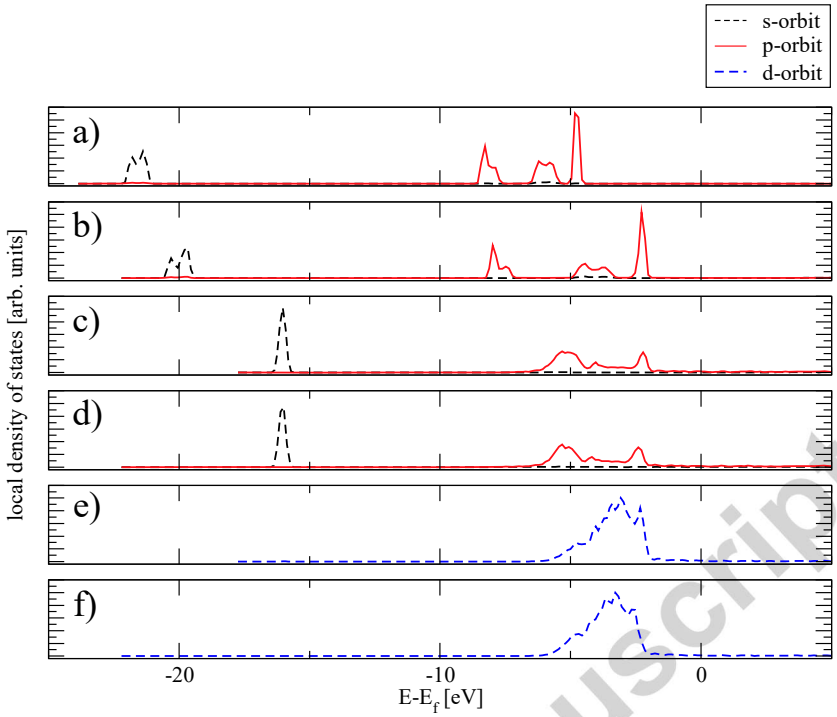

Figure 7: The density of states (LDOS), calculated with the vdW-DF2 for the most stable, type C simulated structure, in which the hydrogens are oriented towards the top Cu-Cl row. The plots show the LDOS for a) and b) the oxygen of the H_2O molecule, c) and d) LDOS for the Cl atom, and e) and f) LDOS for the nearest Cu atoms, without and with the water dimer – surface interaction.

that used here in order to allow direct comparison of the interaction energies. The interaction energies between the water layer and the surface are -0.04 eV (-0.13 eV) for type A, -0.02 eV (-0.11 eV) for type B, and -0.03 eV (-0.11 eV) for type C calculated with the PBE (vdW-DF2). Both methods thus favor configuration A, yet with a narrow margin. The use of vdW-DF2 yields slightly larger interaction energies in all cases. The magnitude of the interaction energy is similar to that on the Cl covered surface.

4. Discussion

The dimensions of the unit cell steer the respective positions of the water molecules; the lower water molecule is oriented so that the hydrogen atom

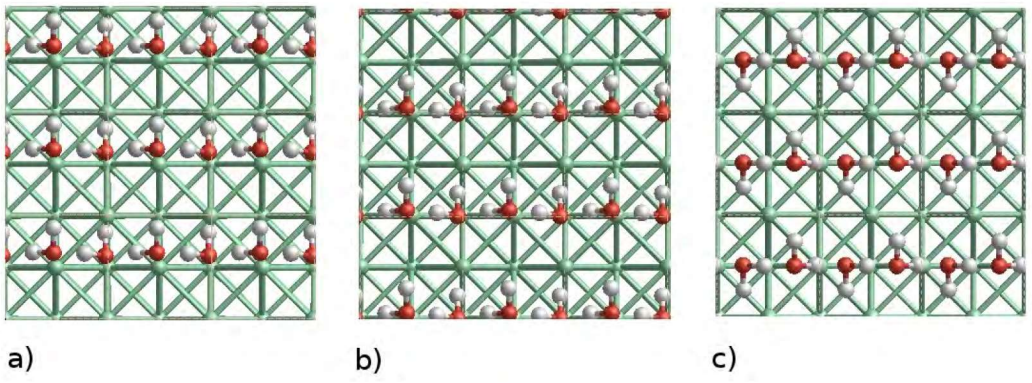

Figure 8: Top views for the models calculated with DFT. Different structure types are: (a) lowermost hydrogen on hollow site (type A), (b) lowermost oxygen on hollow site (type B), and (c) hydrogens alternate from side to side (type C). The color scheme is the same as in figure 4.

is pointing towards the surface. Hamada et al. [26] studied water wetting on Cu(110) surface, and they found that for one water molecule, H-down configuration is not the most favorable adsorption posture. In that sense, the result is consistent with ours. Comparison of the interaction energies on the Cu(100) and the Cu(100)-Cl surface results that the presence of the Cl atom lowers the energy with and without the vdW-DF2 implementation. That might be because the O - Cl interaction is repulsive, since both atoms are strongly electronegative. On the other hand hydrogen atoms, because of their donor nature, bind to both, the O and the surface. At the height where these two interactions balance one another, is the steady adsorption minimum. The PBE and the vdW-DF2 results cannot be compared straightforwardly with each other because of the different lattice constants obtained using these two approximations. Also the lattice mismatch between the water layer and the calculated metal layer causes artificial forces for the water molecules. Nonetheless, the non-local van der Waals interactions drive the adsorption process starting from higher distance. Also the use of vdW-DF2 strengthens the interaction between the water layer and the surface. For the vdW-DF and the PBE, the interaction energy between the water layer and the surface is less than the ice binding energy. The water-water interactions naturally

lead to a zig-zag orientation. The dominance of the water-water interactions over the water layer [U+2013] Cu(100)-Cl interaction therefore enables the formation of zig-zag chains instead of the formation of three dimensional water clusters.

5. Conclusions

We have performed a combined LEED-IV and DFT study for the co-adsorption of chlorine and water on the Cu(100) surface. By interpreting the LEED results using information derived from DFT we conclude that on Cu(100)-Cl water forms a bilayer, the structure of which is dictated by the underlying Cl layer. The DFT results show that the charge transfer between the water bilayer and the surface is negligible, which indicates weak binding between the layer and the surface. This result is also supported by the XPS scans, showing no shifts in the binding energies of the Cu and Cl 2p states.

6. Acknowledgemets

We thank Dr. Andris Gulans for useful discussions. The work was supported in part by the Academy of Finland through grant 135102. We thank the Finnish IT Centre - CSC for providing computational resources.

[1] M. A. Henderson, Surf. Sci. Rep. 46 (2002) 1.

[2] P. A. Thiel, T. E. Madey, Surf. Sci. Rep. 7 (1987) 211.

[3] A. Hodgson, S. Haq, Surf. Sci. Rep. 64 (2009) 381.

[4] J. Carrasco, A. Hodgson, A. Michaelides, Nature Mat. 11 (2012) 667.

[5] S. Schnur, A. Gross, New Journal of Physics 11 (2009) 125003.

[6] D. Westphal, A. Goldmann, F. Jona, P. M. Marcus, Solid State Com. 44 (1982) 685.

[7] D. W. Bullet, Solid State Com. 38 (1981) 969.

[8] H. C. N. Tolentino, Surf. Sci. 601 (2007) 2962.

[9] Y. Grunder, et al, Phys. Rev. B 81 (2010) 174114.

[10] F. Jona, D. Westphal, A. Goldmann, P. M. Marcus, J. Phys. C 16 (1983) 3001.

[11] N. D. Spencer, P. J. Goddard, P. W. Davies, M. Kitson, R. M. Lambert, Journal Vacuum Sci. Tech. A 1 (1983) 1554.

[12] M. A. Van Hove, W. Moritz, H. Over, P. J. Rous, A. Wander, A. Barbieri, N. Materer, U. Starke, G. A. Somorjai, Surf. Sci. Rep. 19 (1993) 191.

[13] A. Barbieri, M. A. Van Hove, private communication.

[14] J. B. Pendry, J. Phys. C 13 (1980) 937.

[15] G. Kresse, J. Hafner, Phys. Rev. B 47 (1993) 558.

[16] G. Kresse, J. Hafner, Phys. Rev. B 49 (1994) 14251.

[17] G. Kresse, J. Furthm[U+00FC]ller, Comp. Mat. Sci. 6 (1996) 15.

[18] G. Kresse, J. Furthmüller, Phys. Rev. B 54 (1996) 11169.

[19] J. P. Perdew, K. Burke, M. Ernzerhof, Phys. Rev. Lett. 77 (1996) 3865.

[20] A. Gulans, M. J. Puska, R. M. Nieminen, Phys. Rev. B 79 (2009) 201105.

[21] M. Dion, H. Rydberg, E. Schröder, D. C. Langreth, B. I. Lundqvist, Phys. Rev. Lett. 92 (2004) 246401.

[22] V. R. Cooper, Phys. Rev. B 81 (2010) 161104.

[23] H. J. Monkhorst, J. D. Pack, Phys. Rev. B 13 (1976) 5188.

[24] G. Woan, The Cambridge Handbook of Physics Formulas, Cambridge University Press, 2000.

[25] J. Klimeš, D. R. Bowler, A. Michaelides, Phys. Rev. B 83 (2011) 195131.

[26] I. Hamada, S. Meng, Chem. Phys. Lett. 521 (2012) 161.

[27] P. J. Feibelman, Phys. Chem. Chem. Phys. 10 (2008) 4688.

[28] G. Henkelman, A. Arnaldsson, H. Jonsson, Comp. Mat. Sci. 36 (2006) 354.

[29] R. F. W. Bader, Atoms in Molecules - A Quantum Theory, Oxford University Press, UK, 1990.

[30] W. Tang, E. Sanville, G. Henkelman, J. Phys.: Condens. Matter. 21 (2009) 084204.

[31] E. Sanville, S. D. Kenny, R. Smith, G. Henkelman, J. Comput. Chem. 28 (2007) 899.